Electronic Supplementary Information

Effects of Intermetal Distance on the Electrochemistry-induced Surface Coverage of M–N–C Dual-Atom Catalysts

Weijie Yang*[a], Zhenhe Jia[a], Liugang Chen[a], Binghui Zhou[a], Di Zhang[b], Yulan Han[c], Zhengyang Gao[a], and Hao Li*[b]

[a] *Department of Power Engineering, School of Energy, Power and Mechanical Engineering, North China Electric Power University, Baoding 071003, China.*

[b] *Advanced Institute for Materials Research (WPI–AIMR), Tohoku University, Sendai 980–8577, Japan.*

[c] *School of Chemistry and Chemical Engineering, Queen's University Belfast, Belfast BT9 5AG, UK.*

Corresponding Author: yangwj@ncepu.edu.cn; li.hao.b8@tohoku.ac.jp

Computational Methods

In this study, all DFT calculations were performed utilizing the Vienna ab initio simulation package (VASP 5.4.4) with the Perdew–Burke–Ernzerhof (PBE) functional and projector-augmented wave (PAW) potentials, which have been demonstrated to be suitable for graphene-based materials. The effects of spin-polarization and van der Waals dispersion were included in the calculations. A 12.33 Å × 12.83 Å graphene with a vacuum layer of 20 Å was modelled to simulate the catalyst surface. In structural optimization, a 2 × 2 × 1 Γ-centred k-point mesh grid and 450 eV energy cutoff were employed. The convergence criteria for energy and force were set to 10^{-5} eV and 0.02 eV/Å, respectively. To achieve higher accuracy, a 4 × 4 × 1 Γ-centred k-point mesh grid was adopted for the subsequent self-consistent field calculations.

To evaluate the stability of DACs, binding energy (E_b), formation energy (E_f), and cohesive energy (E_coh) were calculated. The equations for calculating the E_b, E_f, and E_coh are defined as the following:[1,2,3]

$$E_\mathrm{b} = (E_\mathrm{slab} - E_\mathrm{NC} - \Sigma E_\mathrm{metal}) / 2$$

$$E_\mathrm{f} = E_\mathrm{slab} - x\mu_\mathrm{N} - y\mu_\mathrm{C} - \Sigma\mu_\mathrm{metal}$$

$$E_\mathrm{coh} = \frac{E_\mathrm{metal-bulk}}{n} - E_\mathrm{metal-single}$$

where E_slab, E_NC, and E_metal are the electronic energies of the catalyst, graphene substrate, and metal atoms, respectively. x and y represent the total numbers for N and C, respectively. μ_N and μ_C denote the chemical potentials of N and C atoms, which were obtained from N_2 molecular and pristine graphene, respectively. Considering the impact of temperature and pressure on chemical potential, herein, the energy of N_2 was calculated under the standard state (T = 298.15 K, p = 100 kPa).[6-10] $E_\mathrm{metal-bulk}$ and $E_\mathrm{metal-single}$ represent the metal energies calculated from bulk and a single atom, respectively.

The Gibbs free energy changes (ΔG) of the intermediates were calculated based on the computational hydrogen electrode (CHE) model by Nørskov et al., in which the chemical potential of ($H^+ + e^-$) pair is related to half of the H_2 gas molecule under standard conditions.[4] Therefore, ΔG can be determined using the following equation:

$$\Delta G = \Delta E + \Delta \mathrm{ZP}E - T\Delta S + \Delta G_\mathrm{U} + \Delta G_\mathrm{pH}$$

where ΔE is the difference of electronic energy in the ground state obtained from self-consistent calculations; $\Delta \mathrm{ZP}E$ and ΔS are the difference in zero-point energy and entropy, respectively; T is the temperature (*i.e.*,

298.15 K); ΔG_{U} is the free energy contribution related to the applied potential. ΔG_{pH} is the correction of the free energy of hydrogen ion concentration: $\Delta G_{\mathrm{pH}} = k_B \times T \times \ln 10 \times pH$, where k_B is the Boltzmann constant (8.617343×10^{-5} eV K^{-1}).[5]

Based on the equilibrium between adsorption and aqueous solution, the free energy changes can be determined using the following equation:

$$\Delta G = G_{P^*} + mG_{H_2O} - G_{P-O_mH_n^*} - (2m - n)(0.5G_{H_2} - U_{SHE} - 2.303\, k_B T pH)$$

where G_{P*}, $G_{P-O_mH_{n*}}$, G_{H_2O}, and G_{H_2} are the Gibbs free energies of the pristine surface, coverage surface, H_2O, and H_2, respectively. m and n represent the numbers of O and H in the adsorbate, respectively. U_{SHE} is the potential *vs*. standard hydrogen electrode (SHE).

To describe the capability of attracting electrons of different DACs, the system electronegativity (X) was calculated using the following equation:

$$X = (xX_N + yX_C - \Sigma X_{Metal}) \times \frac{\Sigma \theta_d}{\Sigma n_d}$$

where x and y are the number of N and C adjacent to the embedded metal atom; X_C, X_N and X_{Metal} are the electronegativity of the carbon, nitrogen, and metal atoms, respectively; θ_d is the number of occupied electrons of the *d* orbitals of metal atoms; n_d is the maximum number of electrons in the *d* orbitals.

Table S1. Electronic energies (E) of the species at 298.15 K in this work which applied to calculate the chemical potential. The energy of the gas phase N_2 was calculated under the standard state (T = 298.15 K, p = 100 kPa).[6-10] All values are given in eV.

Species	E (eV)
N_2	-17.05
Graphene (60 C atoms)	-533.40
Fe	-3.46
Co	-1.98

Table S2. Contributions to the adsorption free energy from the zero-point energy corrections, enthalpic (heat capacity) corrections, and entropic corrections. All values are given in eV.

Adsorbate	ZPE	TS	$\int C_P dT$	ΔG
H*	0.219	-0.009	-0.001	0.226
O*	0.084	0.039	0.024	0.069
HO*	0.370	0.078	0.043	0.335

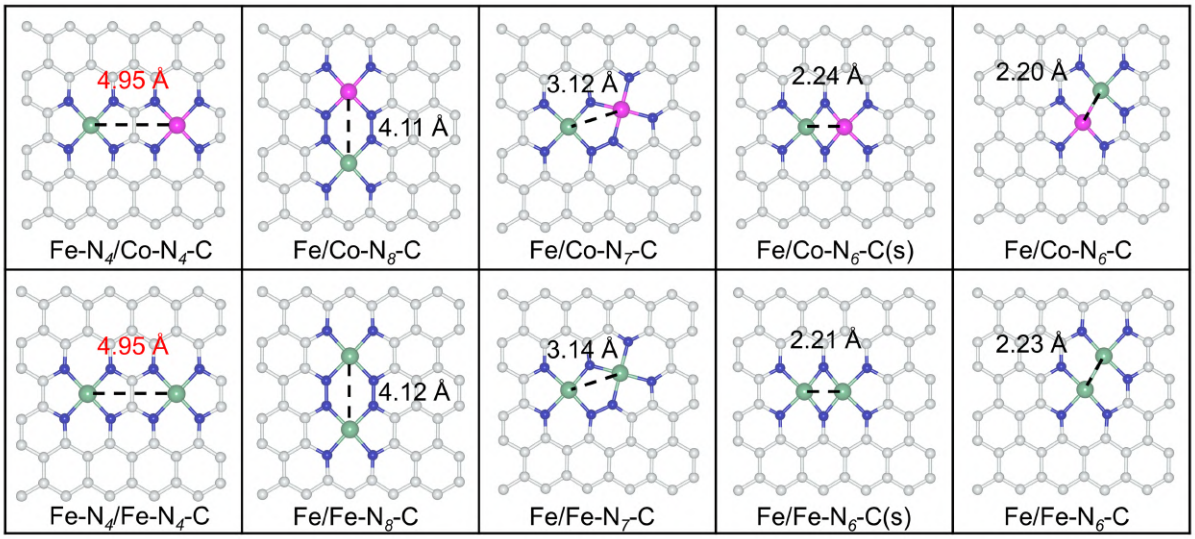

Fig. S1. Geometric configurations of DAC and DAC-like materials, where green, violet, blue, and silvery spheres represent Fe, Co, N, and C, respectively.

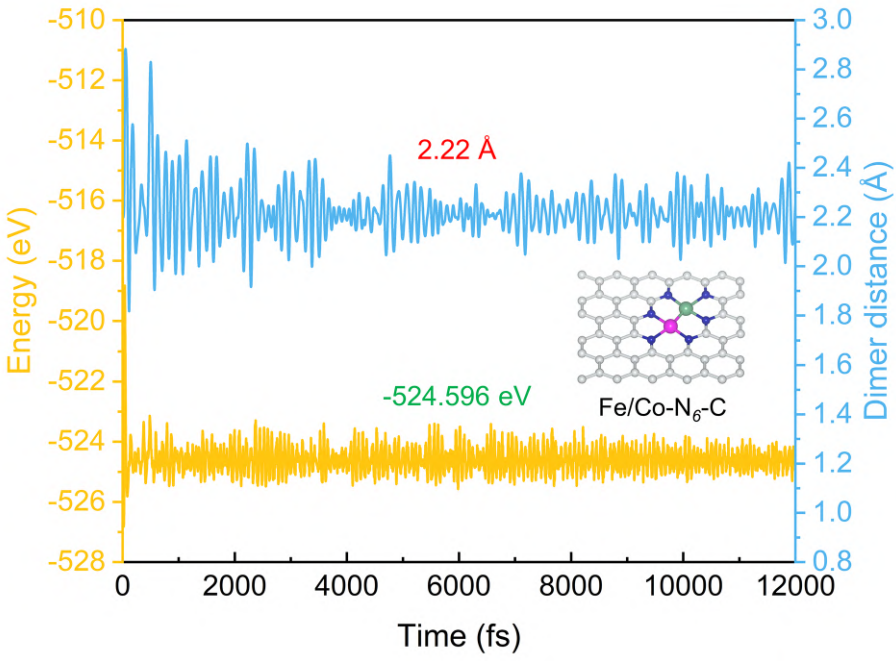

Fig. S2. System energies and the average intermetal distances of Fe/Co-N_6-C during AIMD simulations, where green, violet, blue, and silvery spheres represent Fe, Co, N, and C, respectively.

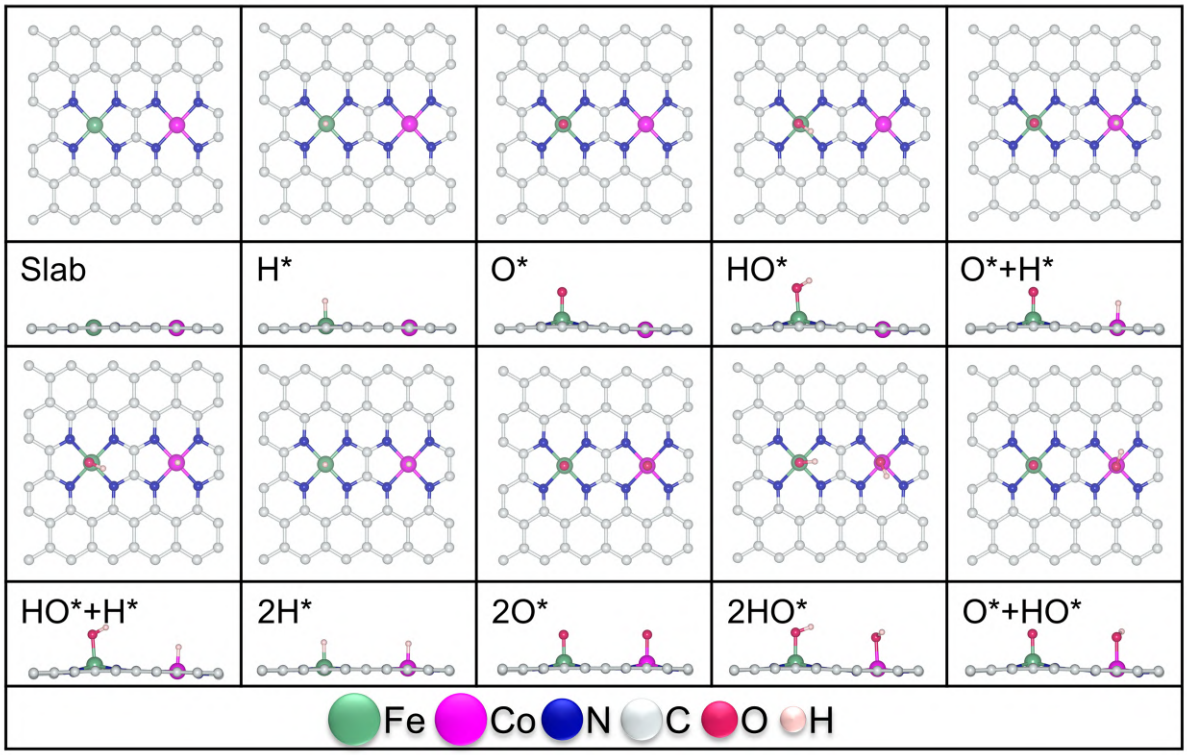

Fig. S3. Adsorption configurations of Fe-N_4/Co-N_4-C where green, violet, blue, silvery, red, and light pink spheres represent Fe, Co, N, C, O, and H, respectively.

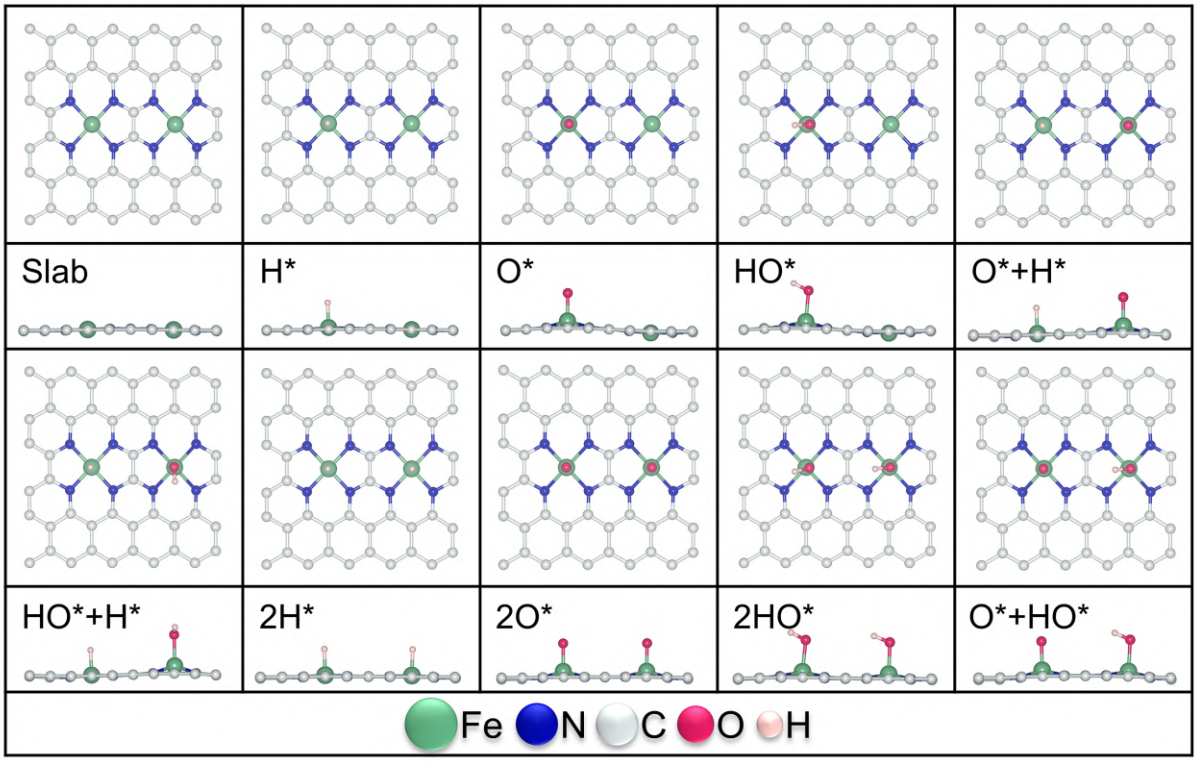

Fig. S4. Adsorption configurations of Fe-N_4/Fe-N_4-C where green, blue, silvery, red, and light pink spheres represent Fe, N, C, O, and H, respectively.

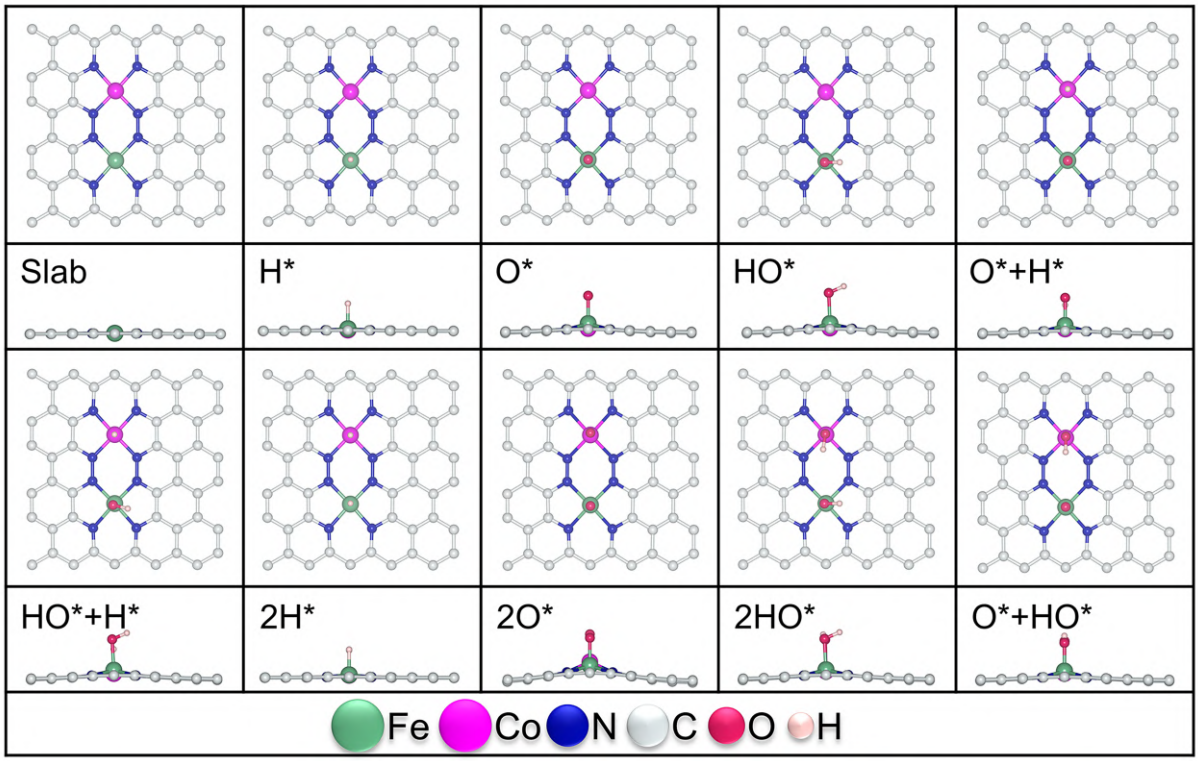

Fig. S5. Adsorption configurations of Fe/Co-N_8-C where green, violet, blue, silvery, red, and light pink spheres represent Fe, Co, N, C, O, and H, respectively.

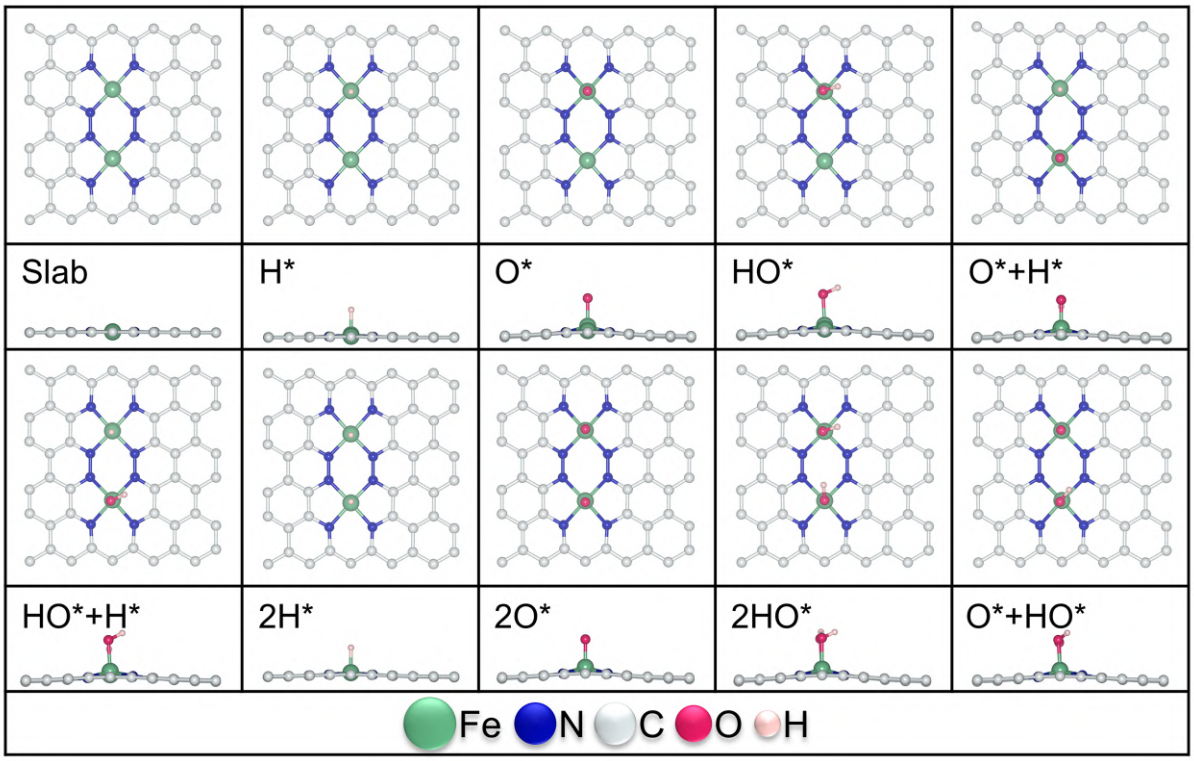

Fig. S6. Adsorption configurations of Fe/Fe-N_8-C where green, blue, silvery, red, and light pink spheres represent Fe, N, C, O, and H, respectively.

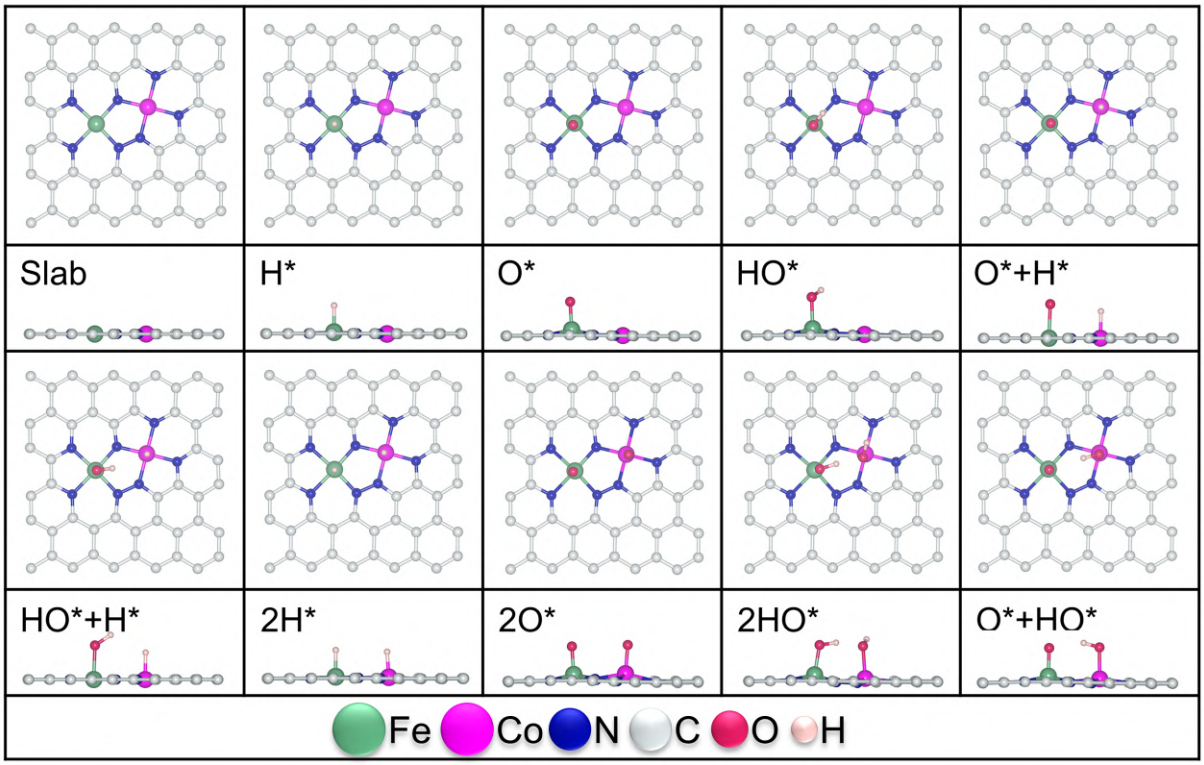

Fig. S7. Adsorption configurations of Fe/Co-N_7-C where green, violet, blue, silvery, red, and light pink spheres represent Fe, Co, N, C, O, and H, respectively.

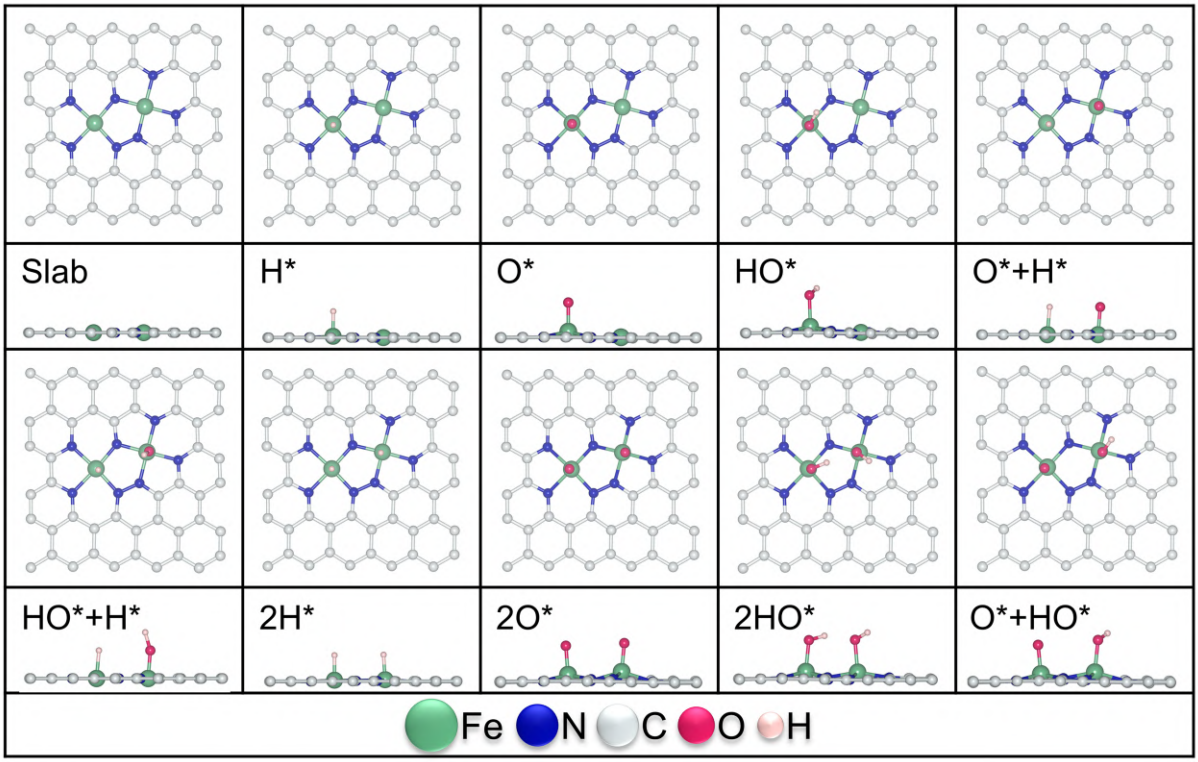

Fig. S8. Adsorption configurations of Fe/Fe-N_7-C where green, blue, silvery, red, and light pink spheres represent Fe, N, C, O, and H, respectively.

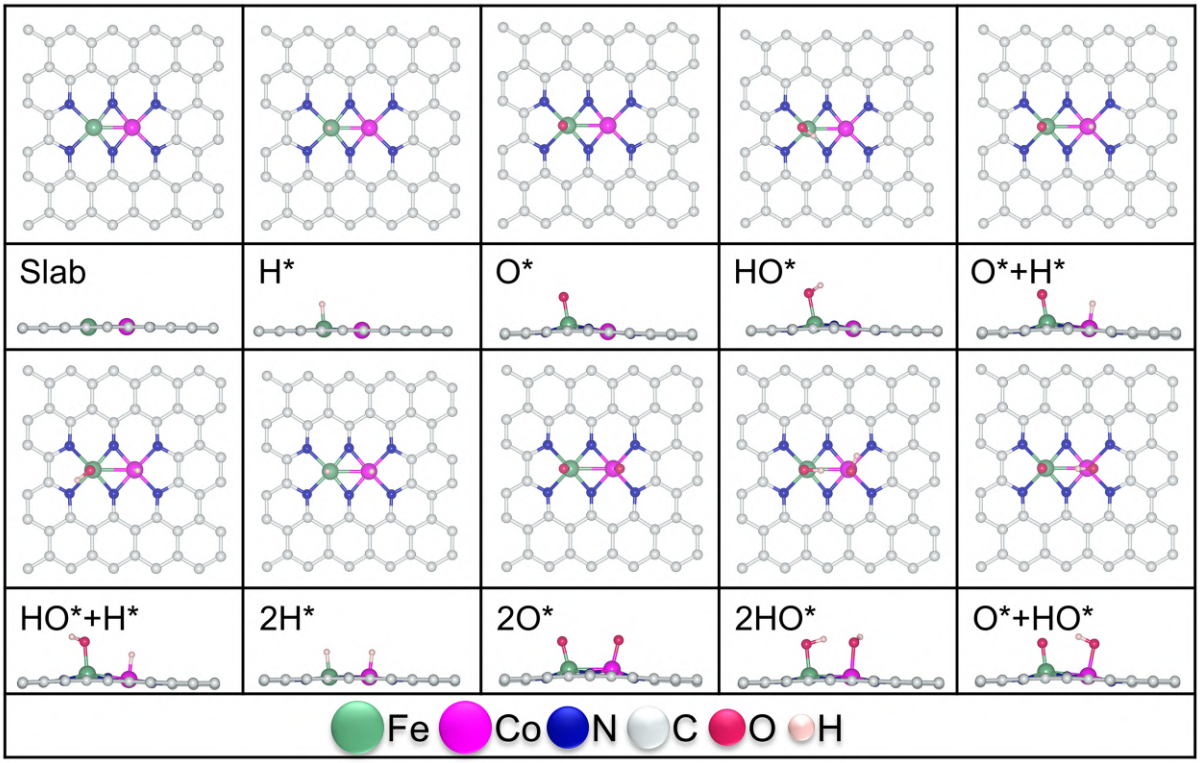

Fig. S9. Adsorption configurations of Fe/Co-N_6-C (s) where green, violet, blue, silvery, red, and light pink spheres represent Fe, Co, N, C, O, and H, respectively.

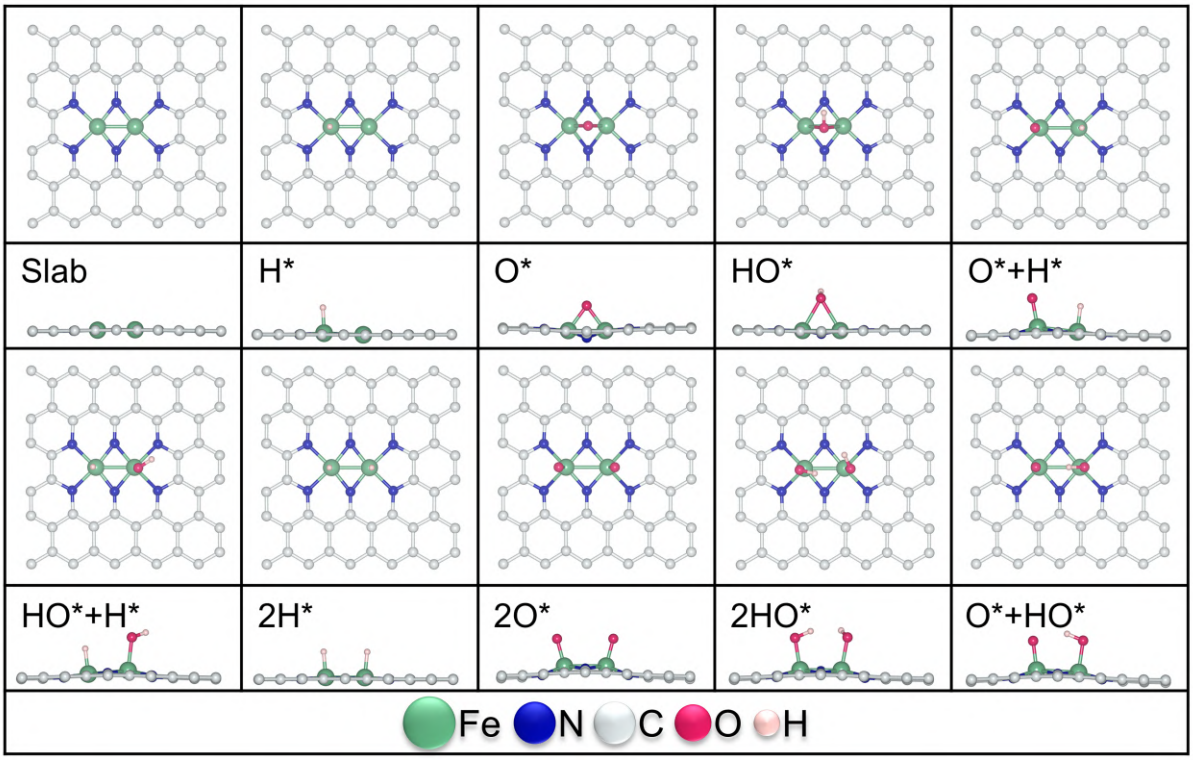

Fig. S10. Adsorption configurations of Fe/Fe-N_6-C (s) where green, blue, silvery, red, and light pink spheres represent Fe, N, C, O, and H, respectively.

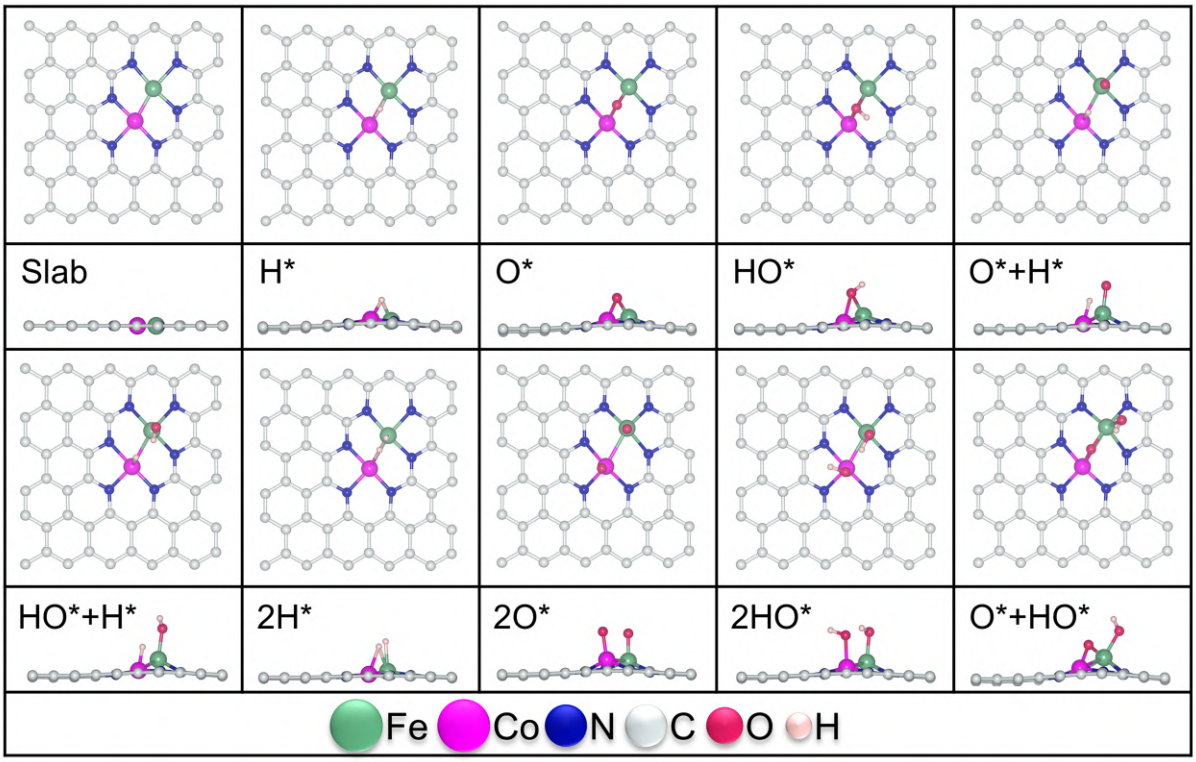

Fig. S11. Adsorption configurations of Fe/Co-N_6-C where green, violet, blue, silvery, red, and light pink spheres represent Fe, Co, N, C, O, and H, respectively.

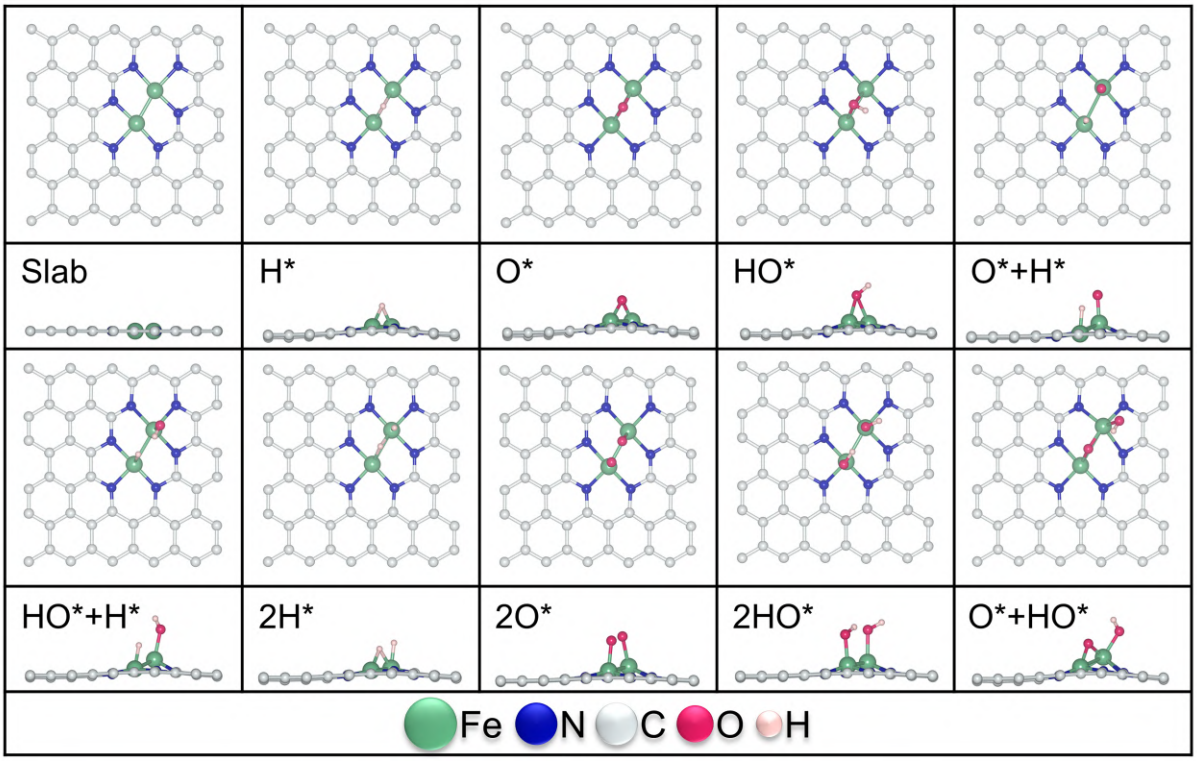

Fig. S12. Adsorption configurations of Fe/Fe-N_6-C where green, blue, silvery, red, and light pink spheres represent Fe, N, C, O, and H, respectively.

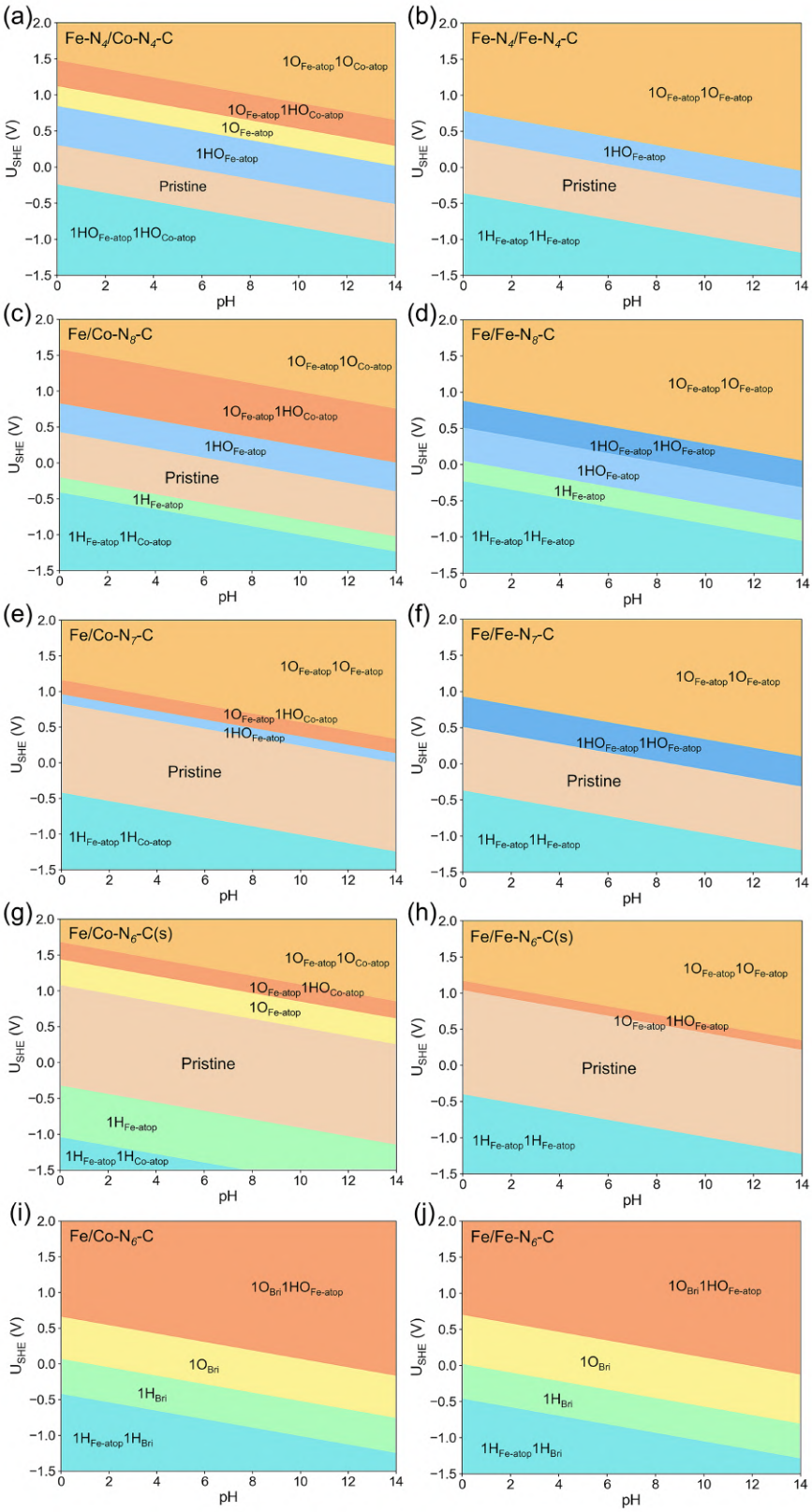

Fig. S13. 2D Surface Pourbaix diagrams of DAC and DAC-like materials as the function of pH and potential. (a-j) Surface Pourbaix diagrams in a wide pH range of (a) Fe-N_4/Co-N_4-C, (b) Fe-N_4/Fe-N_4-C, (c) Fe/Co-N_8-C, (d) Fe/Fe-N_8-C, (e) Fe/Co-N_7-C, (f) Fe/Fe-N_7-C, (g) Fe/Co-N_6-C (s), (h) Fe/Fe-N_6-C (s), (i) Fe/Co-N_6-C, and (j) Fe/Fe-N_6-C.

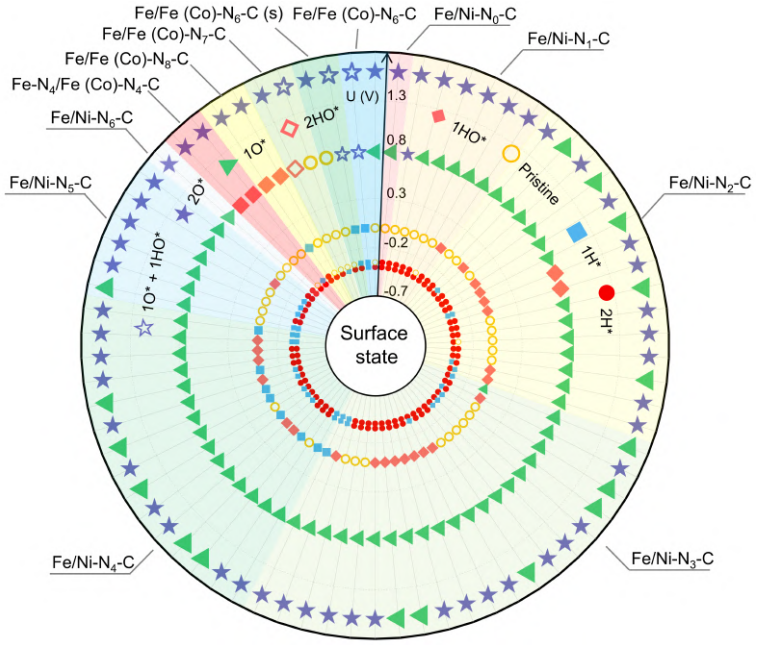

Fig. S14. Identified electrochemistry-induced surface coverages of DACs at the characteristic potentials of HER (0 V_{RHE}), OER (1.60 V_{RHE}), ORR (0.78 V_{RHE}), CO_2RR (−0.35 V_{RHE}), and NRR (−0.40 V_{RHE}).

References

1. X. Zheng, Y. Yao, W. Ye, P. Gao, Y. Liu, *Chem. Eng. J.*, 2021, **413**, 128027.
2. Y. Meng, K. Li, D. Xiao, Y. Yuan, Y. Wang, Z. Wu, *Int. J. Hydrogen Energy*, 2020, **45**, 14311-14319.
3. P. Janthon, S. M. Kozlov, F. Vines, J. Limtrakul, F. Illas, *J. Chem. Theory Comput.*, 2013, **9**, 1631-1640.
4. A. A. Peterson, F. Abild-Pedersen, F. Studt, *Energy. Environ. Sci.*, 2010, **3**, 1311–1315.
5. W. Yang, X. Chen, Y. Feng, F. Wang, Z. Gao, Y. Liu, H. Li, *Environ. Sci-Nano*, 2022, **9**, 2041-2050.
6. L. Li, R. Huang, R., X. Cao, Y. Wen, *J. Mater. Chem. A*, 2020, **8**, 19319-19327.
7. G. Xiao, R. Lu, J. Liu, X. Liao, Z. Wang, Y. Zhao, *Nano. Res*., 2022, **15**, 3073–3081.
8. N. Yang, X. Zheng, L. Li, *J. Phys. Chem. C*, 2017, **121**, 19321-19328.
9. Y. Yang, H. Zhang, Z. Liang, Y. Yin, B. Mei, *J. Energy Chem*., 2020, **44**, 131-137.
10. X. Guo, J. Gu, S. Lin, *J. Am. Chem. Soc*., 2020, **142**, 5709-5721.